

KH130405 final report
The origin of the elements heavier than iron

Context: Within this project we have investigated predominantly Barium (Ba) stars, which are stars polluted by material enriched in the elements heavier than iron produced by the *slow* neutron capture process (the *s*-process) in the interior of their former asymptotic giant branch (AGB) companion star, which is now a white dwarf. We have also used Ba stars to understand the origin of meteoritic stardust grains, and we have developed new models of *intermediate* neutron captures (the *i* process) to investigate the puzzling Pd depletion in post-AGB stars located in the Magellanic Clouds. We also modelled the evolution of the Milky Way Galaxy of all the elements from C to U from first principles, and the nature of specific stars that are currently producing heavy elements (the supergiant Betelgeuse) or will evolve into AGB stars (Cepheids and RR Lyrae).

In Cseh, Vilagos¹ et al. (in preparation), we have compared individual Ba star abundance patterns to AGB nucleosynthesis model predictions to verify if the AGB model mass for each star is compatible with the AGB mass previously and independently estimated using binary parameters and parallax data from the Gaia satellite, and via positioning the star on the HR diagram and comparing with evolutionary tracks. We selected the sample of 28 Ba stars for which both self-consistent spectroscopic observations and analysis and binary-derived stellar mass determination are available. For this sample stars we considered both previously (Y, Zr, Ce, and Nd) and recently (Rb, Sr, Nb, Mo, Ru, La, Sm, and Eu) derived elemental abundances (by Roriz, Lugaro et al., 2021a,b published papers described below). Then, we performed a detailed comparison between these *s*-process elemental abundances and different AGB nucleosynthesis models, of the corresponding mass and metallicity (Fe/H) from each star, from the Monash and the FRUITY theoretical data sets. We simplified the binary mass transfer by calculating dilution factors to match the Ce/Fe value of each star when using different AGB nucleosynthesis models, and we then compared the diluted model abundances to each complete Ba-star abundance pattern. Our comparison confirms that low-mass (roughly in the range 2-3 M_{\odot}), non-rotating AGB stellar models with the $^{13}\text{C}(\alpha, n)^{16}\text{O}$ reaction as the main neutron source are the polluters of the vast majority of the considered Ba stars. Out of the 28 stars, in 21 cases the models are in good agreement with both the determined abundances and the binary-derived AGB mass (see example in Figure 1). However, in 16 cases higher observed abundances of Nb, Ru, Mo and/or Nd, Sm than predicted (see example in Figure 2). For 3 stars we obtain a match to the abundances only by considering models with masses lower than those independently determined. Finally, 4 stars show much higher first *s*-process peak abundance values than the model predictions, which may represent the signature of a physical (e.g., mixing) and/or nucleosynthetic process that is not represented in the set of models we have considered.

In the two papers by Roriz, Lugaro et al. 2021 (published in MNRAS) we collaborated with colleagues in Brazil to publish and compare to the models² abundances for many elements derived for a large sample of 180 Ba stars. These were observed in the optical with the Fiber-fed Extended Range Optical Spectrograph (FEROS) at the 1.52 m and 2.2 m ESO telescopes. One of the main element is rubidium (Rb), which is key for the *s*-process diagnostic because it is sensitive to the neutron density and hence its abundance points to the main neutron source of the *s*-process in AGB stars and the mass of the star. We compare the observed Rb/Zr ratios with theoretical predictions from *s*-process models in AGB stars.

¹ Blanka Világos was hired as a student demonstrator and she won the first prize at the OTDK (National Scientific Students' Association Conference) in 2021 with a project based on this paper.

² Note that in these Roriz et al. papers we presented the new observations and discussed their comparison to the models for the Ba-star stellar population as a whole. In the Cseh et al. paper in preparation described above, instead, we compared the models to each individual star of the 28 with available binary mass determination, one by one. In Den Hartog et al. (in preparation) we are extending this analysis to the total sample of ~180 Ba stars of Roriz et al., using machine learning techniques to be able to compare the data to the models given the large sample

The Ba stars display $Rb/Zr < \text{solar}$, showing that Rb was not efficiently produced by the activation of the branching points at ^{85}Kr and ^{86}Rb . Model predictions from the Monash and FRUITY datasets of low-mass ($\lesssim 4 M_{\odot}$) AGB stars are able to cover the Rb abundances observed in the program Ba stars. These observations indicate that the $^{13}\text{C}(\alpha, n)^{16}\text{O}$ reaction is the main neutron source of the s -process in the low-mass AGB companions of the observed Ba stars. We have not found in the present study candidate companions for former IR/OH massive AGB stars, which are observed to have $Rb/Zr > \text{solar}$ instead. We also presented the elements Sr, Nb, Mo, Ru, La, Sm, and Eu, as derived by equivalent width measurements or synthetic spectra computations and compared them with available data for field giant and dwarf stars in the same range of metallicity. A re-determination of La abundances resulted in La/Fe ratios up to ten times lower than values previously reported in literature. The Ba stars show overabundance of neutron-capture elements, except for Eu, for which the observational data set behave similarly to field stars. Comparison to model predictions are satisfactory for second-to-first s -process peak ratios (e.g., Ce/Y), which are both observed and predicted to decrease as the metallicity increases, and the ratios of the predominantly rapid neutron capture (r -process) element Eu to La. However, the observed Nb, Mo, Ru/Sr and Ce, Nd, Sm/La ratios show median values higher or at the upper limits of the ranges of the model predictions. This unexplained feature is confirmed by the comparison of the models to each individual star (see above, and Figure 2) and calls for new neutron-capture models to be investigated.

In Lugaro, Cseh, Világos et al. 2020 (ApJ) we used the Ba stars data to understand the origin of stardust grains that are produced in AGB stars. We presented evidence that the majority of large (μm -sized) meteoritic silicon carbide (SiC) grains formed in C-rich AGB stars that were more metal-rich than the Sun. In the framework of the s process in AGB stars, the lower-than-solar $^{88}\text{Sr}/^{88}\text{Sr}$ isotopic ratios measured in the large SiC grains can only be accompanied by Ce/Y elemental ratios that are also lower than solar and, as mentioned above, predominantly observed in Ba stars that are more metal rich. Such an origin suggests that these large grains represent the material from high-metallicity AGB stars needed to explain the s -process nucleosynthesis variations observed in bulk meteorites. We also show that in the outflows of metal-rich, C-rich AGB stars, SiC grains are predicted to be small ($\sim 0.2 \mu\text{m}$); large ($\sim \mu\text{m}$ -sized) SiC grains can grow if the number of dust seeds is 2–3 orders of magnitude lower than the standard value of 10^{13} times the number of H atoms. We therefore predict that with increasing metallicity, the number of dust seeds might decrease, resulting in the production of larger SiC grains.

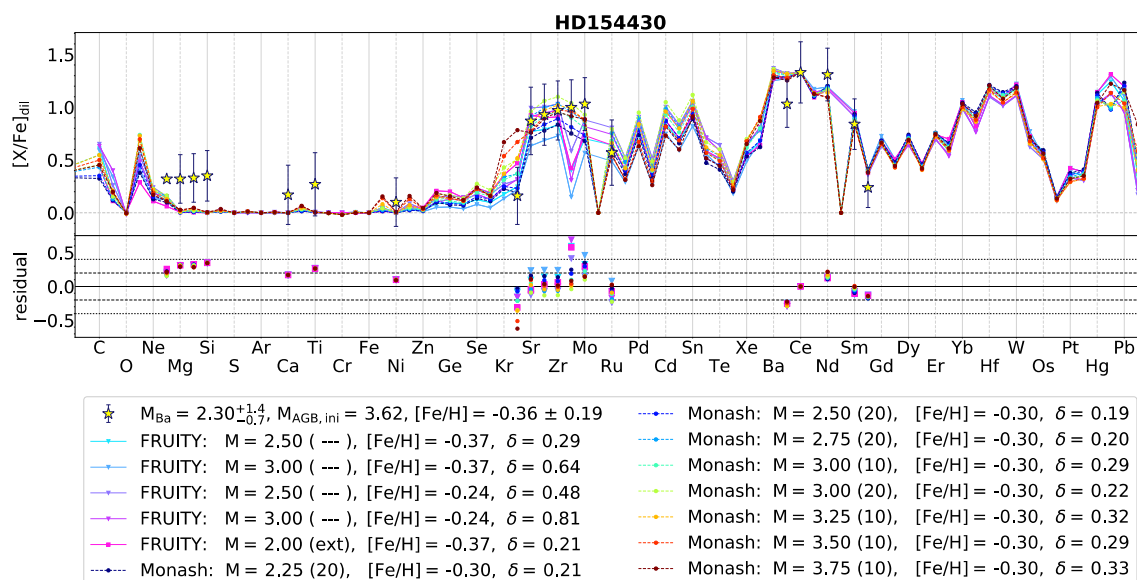


Figure 1. Comparison of a Ba star with AGB models. This star shows a typical s -process abundance pattern that can be well explained by the models, with the relative abundances at the second (e.g., Ce) and first (e.g., Y) s -process peaks well reproduced by models of the same metallicity as observed in the star, and a flat pattern of abundances for Sr to Mo. In this and the next figures the notation $[X/\text{Fe}]$ represent the Log_{10} of the stellar abundance ratio X/Fe (where X is a generic element) divided by the solar abundance ratio.

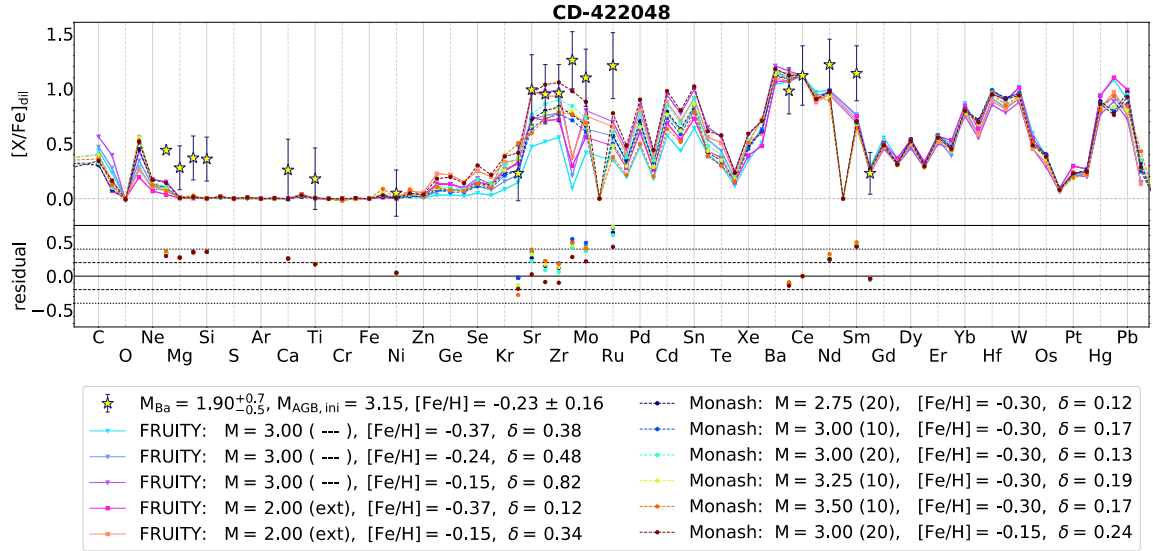


Figure 2. Same as Figure 1: the second to first peak relative abundances are well reproduced, however, this Ba star shows excesses in the elements Nb, Mo, Ru (after the first peak) and Nd, and Sm (after the second peak), which cannot be explained by the current models.

To further investigate dust formation, in Ventura et al. (2020, 2021, published in A&A) we presented dust production in AGB models with super-solar and very low metallicities, respectively in the two papers. We found that most of the dust produced by the metal-rich AGB stars is in the form of silicate particles and that the total mass of dust produced increases with the mass of the star, reaching up to $\sim 0.012 M_{\odot}$ for star of initial mass of $8 M_{\odot}$. For the very low metallicity (10^{-5} and 10^{-7} solar) models, we found that stars of mass $< 2 M_{\odot}$ produce significant quantities of carbonaceous dust, of the order of $0.01 M_{\odot}$, while little dust production takes place in their winds of stars of mass $> 5 M_{\odot}$ stars.

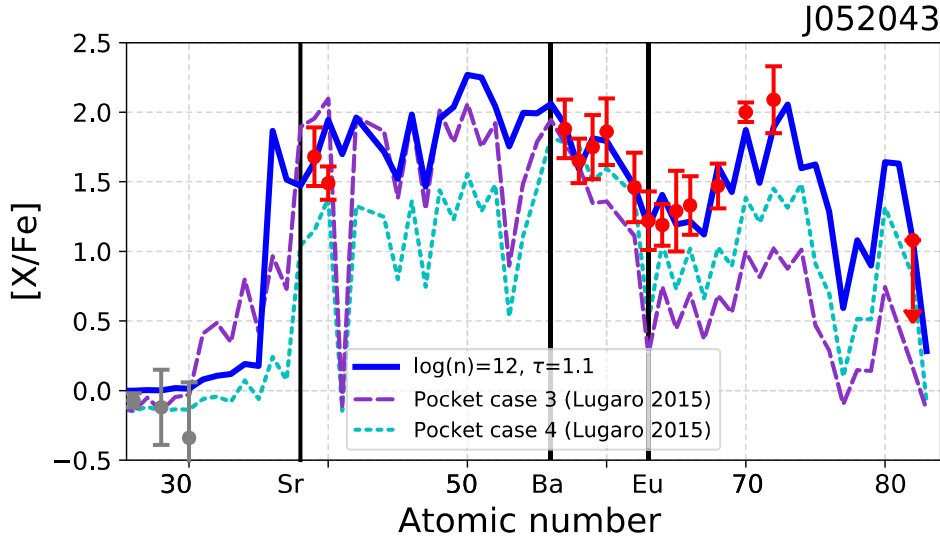


Figure 3. Comparison between the composition of a post-AGB star in the Magellanic Clouds and models of the *s* (purple dashed line and dotted cyan line) and the *i* process (blue solid line). The *s*-process models cannot match the observed low Pb abundance together with the high abundances of the elements just after Eu. Models of the *s* process not shown in the figure can match the abundances of these elements; however, they predict a value of $[Pb/Fe]$ above 2.

In Hampel et al. (2019, ApJ), we investigated the nature of post-AGB stars, of initial mass around $1 M_{\odot}$ and metallicity roughly $1/10^{\text{th}}$ of solar, in the Magellanic Clouds, which have puzzlingly low Pb abundances. Lead (Pb) is predominantly produced by the *s* process in AGB stars. In contrast to significantly enhanced Pb abundances predicted by the corresponding low-mass, low-metallicity AGB models, observations of these post-AGB stars in the Magellanic Clouds show incompatibly low Pb

abundances. Observations of carbon-enhanced metal-poor (CEMP) stars whose *s*-process enrichments are accompanied by heavy elements traditionally associated with the *rapid* neutron-capture process (the *r* process) have raised the need for a neutron-capture process operating at neutron densities *intermediate* to the *s* and *r* process: the so-called *i* process. We found that our *i*-process models can explain the heavy-element abundance patterns measured in the post-AGB stars including their puzzlingly low Pb abundances (see Figure 3). Furthermore, the heavy-element enhancements in the post-AGB and CEMP-*i* stars, particularly their Pb abundance, allowed us to characterize the neutron densities and exposures of the *i* process that produced the observed abundance patterns. We find that the lower-metallicity CEMP-*i* stars (of metallicity ~ 0.01 solar) have heavy-element abundances best matched by models with higher neutron densities and exposures as compared to the higher-metallicity post-AGB stars (of metallicity ~ 0.1 solar). This offers new constraints and insights regarding the properties of *i*-process sites and demonstrates that the responsible process operates on timescales of the order of a few years or less.

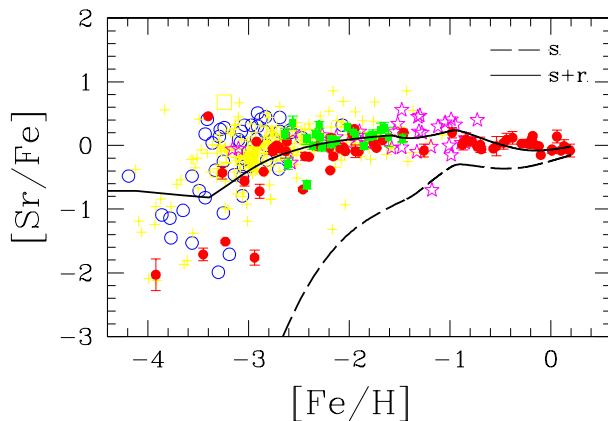


Figure 4. The evolution of Sr/Fe for the solar neighbourhood as function of time, represented by the evolution of [Fe/H], in the GCE models with the *s* process only (dashed line) and the *s+r* processes included (solid line). The coloured observational data points are from different sources.

abundances of the second (Ba) and third (Pb) peak elements are well reproduced with our updated yields of *s* process from AGB stars. The first peak elements (Sr, Y, Zr, e.g., Figure 4) are sufficiently produced by electron-capture supernovae together with AGB stars. Neutron star mergers can produce the *r*-process elements up to Th and U, but the timescales are too long to explain observations at low metallicities. The observed evolutionary trends, such as for Eu, can well be explained if $\sim 3\%$ of 25–50 M_{\odot} stars explode as magneto-rotational supernovae producing *r*-process elements. Note that our team was also involved in the ESA Gaia satellite early Data Release 3, which reported new observations for millions of stars in the Milky Way galaxy. These data are essential to constrain, e.g., binary evolution and galactic chemical evolution models.

As the nearby red supergiant³ Betelgeuse mysteriously dimmed between the end of 2019 start of 2002, we took the opportunity in Joyce et al. (2020) to conduct a rigorous examination of this star by drawing on the synthesis of new observational data and three different modelling techniques. New processed photometric measurements were published, as collected with the space-based Solar Mass Ejection Imager instrument prior to Betelgeuse's recent, unprecedented dimming event. The first radial overtone in the photometric data was reported, with a period of 185 ± 13.5 days. The theoretical predictions include self-consistent results from multi-timescale evolutionary, oscillatory, and hydrodynamic simulations conducted with the Modules for Experiments in Stellar Astrophysics software suite. We derived a precise prediction for the stellar radius ($\sim 764 R_{\odot}$), a new, independent distance estimate (~ 168

In Kobayashi, Karakas, and Lugaro (2020, ApJ) we constructed galactic chemical evolution (GCE) models for all stable elements from C ($A=12$) to U ($A=238$) from first principles, i.e., using theoretical nucleosynthesis yields and event rates of all chemical enrichment sources. This enabled us to predict the origin of elements as a function of time (see, e.g., the example of Sr in Figure 4). We find that the contribution to GCE from super-AGB stars (with masses ~ 8 – $10 M_{\odot}$ at solar metallicity) is negligible, unless hybrid white dwarfs from low-mass super-AGB stars explode as so-called Type Ia supernovae, or high-mass super-AGB stars explode as electron-capture supernovae. Among neutron-capture elements, the observed

³ Supergiant stars are expected to explode as core-collapse supernovae and eject heavy elements.

pc), and a parallax of 5.95 mas, in good agreement with Hipparcos. Seismic results from both perturbed hydrostatic and evolving hydrodynamic simulations constrain the period and driving mechanisms of Betelgeuse's dominant periodicities in new ways. We conclude that Betelgeuse's ≈ 400 day period is the result of pulsation in the fundamental mode. Grid-based hydrodynamic modelling reveals that the behaviour of the oscillating envelope is mass-dependent, and likewise suggests that the nonlinear pulsation excitation time could serve as a mass constraint. Our results place this star definitively in the early core helium-burning phase of the red supergiant branch, during which the $^{22}\text{Ne}(a,n)^{25}\text{Mg}$ reaction is activated and the s process occurs in the core. We report a present-day mass of $16.5\text{--}19 M_{\odot}$ - slightly lower than typical literature values.

Finally, in Plachy et al. 2021 and the review by Plachy & Szabó (2021) we have considered giant variable stars (Cepheids and RR Lyrae, respectively in the two papers) that are the evolutionary phases prior of AGB stars and analysed their pulsating features. The first analysis of 35 Cepheid stars from the Galactic field and from the Magellanic Clouds observed by the TESS space mission was presented with the goal to explore the potential and the limitations of TESS concerning the various subtypes of Cepheids. Precise light-curve shapes will be crucial not only for classification purposes but also to determine the physical properties of these stars. In the review on RR Lyrae, the new and unpredicted phenomena that reformed and invigorated RR Lyrae star research are presented as discovered by the unprecedented photometric precision along with the quasi-continuous sampling provided by the *Kepler* space telescope. Specifically, the discovery of period doubling and the wealth of low-amplitude modes enlightened the complexity of the pulsation behaviour. Searching and providing theoretical explanation for these newly found phenomena as well as understanding their connection to the oldest enigma of RR Lyrae stars, the Blazhko effect, are central questions. The challenges of *Kepler* photometry that played a crucial role in these results are also discussed.